Strong synergistic interactions in zwitterionic–anionic surfactant mixtures at the air–water interface and in micelles: The role of steric and electrostatic interactions

Kun Ma, Peixun Li, Zi Wang, Yao Chen, Mario Campana, James Doutch, Robert Dalgliesh, Armando Maestro, Robert K Thomas, Jeff Penfold

Published version information

Citation: K Ma et al. Strong synergistic interactions in zwitterionic–anionic surfactant mixtures at the air–water interface and in micelles: The role of steric and electrostatic interactions. J Coll Int Sci 613 (2022): 297-310. DOI: 10.1016/j.jcis.2022.01.045

Strong synergistic interactions in zwitterionic–anionic surfactant mixtures at the air-water interface and in micelles: the role of steric and electrostatic interactions.

Kun Ma[1], Peixun Li[1], Zi Wang[1,2], Yao Chen[1], Mario Campana[1], James Doutch[1], Robert Dalgliesh[1], Armando Maestro[3,5], Robert K Thomas[4], Jeff Penfold[1,4•]

1. ISIS Facility, Rutherford Appleton Laboratory, STFC, Chilton, Didcot, OXOX, OX11 0QX, UK
2. School of Science, State Key Laboratory of Heavy Oil Processing, China University of Petroleum, Qingdao. 266580. China
3. Institute Laue Langevin, 71 Avenue Des Martyrs, CS 20156, 38042 Grenoble, Cedex 9, France
4. Physical and Theoretical Chemistry Laboratory, University of Oxford, South Parks Road, Oxford, OX1 3QZ, UK
5. Centre de Fisica de Materailes (CSIC, UPV/EHU), Materials Physics centre, Pasco Manuel de Lardizabel 5, E-20018, San Sebastian, Spain; IKERBASQUE, Basque Foundation for Science, Plaza Euskadi 6, Bilbao, 48009, Spain

- Corresponding Author: Jeff Penfold, jeff.penfold@stfc.ac.uk

ABSTRACT.

Hypothesis: The milder interaction with biosystems makes the zwitterionic surfactants an important class of surfactants, and they are widely used in biological applications and in personal care formulations. An important aspect of those applications is their strong synergistic interaction with anionic surfactants. It is anticipated that the strong interaction will significantly affect the adsorption and self-assembly properties.

Experiments: Surface tension, ST, neutron reflectivity, NR, and small angle neutron scattering, SANS, have been used here to explore the synergistic mixing in micelles and at the air-water interface for the zwitterionic surfactant, dodecyldimethylammonium propanesulfonate, C_{12}SB,

and the anionic surfactants, alkyl ester sulfonate, AES, in the absence and presence of electrolyte, 0.1 M NaCl.

Findings: At the air-water interface the asymmetry of composition in the strong synergistic interaction and the changes with added electrolyte and anionic surfactant structure reflect the relative contributions of the electrostatic and steric interactions to the excess free energy of mixing. In the mixed micelles the synergy is less pronounced and indicates less severe packing constraints. The micelle structure is predominantly globular to elongated, and shows a pronounced micellar growth with composition which depends strongly upon the nature of the anionic surfactant and the addition of electrolyte.

INTRODUCTION.

Zwitterionic surfactants are an important class of surfactants (1-6). Their lack of overall charge, in the absence of added electrolyte and at neutral pH, results in a weaker interaction compared to ionic surfactants with a range of biosystems. The milder bio-interaction and associated lower toxicity and improved biodegradability results in their wider and increasing use in home care (5) and personal care (7) products, with the associated reduced eye and skin irritation, in agrochemical formulations involving pesticides, herbicides, defoliants and fertilisers (8), biotechnology (9), as foam boosters (10), in catalysis (11) and enhanced oil recovery (12).

Although the zwitterion is overall neutral, the existence of separate charges makes the surfactant highly water soluble. The presence of discreet charges also results in strong synergistic interactions with ionic surfactants, and is the key to many of the applications and the associated formulations. The synergistic interactions have been extensively studied and characterised (10, 13-23). The strength of the synergistic interaction depends upon the nature of the cosurfactant and on the zwitterionic headgroup structure. The synergistic interaction is strongest with anionic surfactants, and less pronounced for cationic and nonionic surfactants (18, 21, 22). The headgroup structure of the zwitterionic surfactant is important; and, for example, the synergy is more pronounced for sulfobetaine than for carboxyl headgroups (23).

Quantifying the synergistic mixing usually relies on the application of the thermodynamics of mixing, through the Regular Solution Theory, RST, or the more general Pseudo Phase Approximation, PPA, approach, but is often limited in applicability to surface tension, ST, data (12, 14, 20-22). An alternative approach, using the Molecular Thermodynamics method and related approaches, in which the molecular interactions are modelled within a thermodynamics framework, has also been widely applied and specifically to zwitterionic – ionic surfactant

mixtures (10, 24-26). However, the introduction of neutron scattering techniques, which in combination with H/D isotopic substitution, enables surface compositions below and above the critical micelle concentration, cmc, to be directly determined for multi-component mixtures, and micelle compositions to be determined (27, 28), and provides a more detailed evaluation of the surfactant mixing. In combination with ST data this enables a more rigorous and detailed application of the PPA (29). In particular this approach demonstrated the need to include higher order terms in the expansion of the excess free energy of mixing, ΔG^e, to account for the intrinsic asymmetry in the mixing properties. This has now been powerfully demonstrated in a range of binary ionic – nonionic surfactant mixtures, multi-component surfactant mixtures and in zwitterionic – ionic surfactant mixtures (21, 29-31). Through changes in molecular structure and with the addition of electrolyte, the relative contributions of the steric and electrostatic interactions were identified (31). This is the approach used in this paper to study the surface and micelle mixing of the zwitterionic surfactant dodecyldimethylammonium propane sulfonate, C_{12}SB, with different alkyl ester sulfonate, AES, anionic surfactants.

Li et al (21) have recently used this approach to determine and analyse the mixing properties at the air-water interface for C_{12}SB and the anionic surfactant sodium dodecylsulfate, SDS. They showed that the expansion of the ΔG^e up to and including the quartic term was necessary to account for the asymmetry in the adsorbed layer and micelle mixing. For the surface adsorption the minimum in ΔG^e occurred at a surface mole fraction $x_{sds} \sim 0.38$ with a depth ~ -2.8 RT. In the micelles the interaction was weaker with a $\Delta G^e \sim$ -2.2 RT and was more asymmetrical with $x_{sds} \sim 0.23$. The differences in the strength of the synergistic interaction and the composition corresponding to the minimum reflect the differences in the relative contributions of the electrostatic and steric components to the interaction. The relative variations in the surface and micelle packing resulted in a pronounced synergy in the total adsorption, and is associated with changes in the headgroup conformation of the zwitterion on mixing.

The purpose of this paper is to explore how changing the structure of the anionic surfactant and the addition of electrolyte changes the mixing properties and the relative steric and electrostatic contributions to the mixing properties with C_{12}SB. In particular the focus is on the alkyl ester sulfonate surfactants, where compared to SDS the headgroup structure changes from sulfate to methyl ester sulfonate, and the alkyl chain length from dodecyl to tetradecyl and hexadecyl, through the use of sodium tetradecanoic-2-sulfo-1-methyl ester, C_{14}MES, and C_{16}MES. In the context of biosustainability and more environmentally tolerant surfactant based formulations,

the alkyl ester sulfonates are potentially important surfactants. They have enhanced biodegradability, better properties at low temperatures, better tolerance to hard water, and are potentially biosustainable (33). As such their adsorption and self-assembly properties have been extensively explored (34-36). In terms of formulations they have the potential to be an important complement in mixtures and applications involving zwitterionic surfactants. Hence in this paper the surface and micelle mixing properties for C_{12}SB with C_{14}MES and C_{16}MES, with and without electrolyte, are explored using NR, SANS and ST. The results are analysed using recent developments of the PPA, in which ΔG^e is expanded to include quartic and cubic terms in addition to the more established quadratic term (Regular solution approach). The aim is to provide a greater insight into the factors which affect the interaction of anionic surfactants with the zwitterionic betaine surfactant, and how the different electrostatic and steric contributions affect the surface and micelle mixing properties. As such the results should provide an important guide to the complex formulation of products involving zwitterionic surfactants.

EXPERIMENTAL DETAILS

(a) Materials and Methods

(i) Sample Synthesis and Details

The different surfactants used in the ST, NR and SANS measurements were dodecyldimethyl ammonium propane sulfonate, C_{12}SB, with alkyl chain hydrogenous or deuterium labelled, h-C_{12}SB and d-C_{12}SB, sodium tetradecanoic-2-sulfo-1-methyl ester, C_{14}MES, with the alkyl chain deuterium labelled or hydrogeneous, d-C_{14}MES or h-C_{14}MES, the hexadecanoic equivalent, C_{16}MES, in deuterated and hydrogeneous forms, h-C_{16}MES and d-C_{16}MES, sodium tetradecanoic-2-sulfo-1-ethyl ester, C_{14}EES, in hydrogeneous form only, h-C_{14}EES. The structures of the different surfactants are illustrated in figure 1.

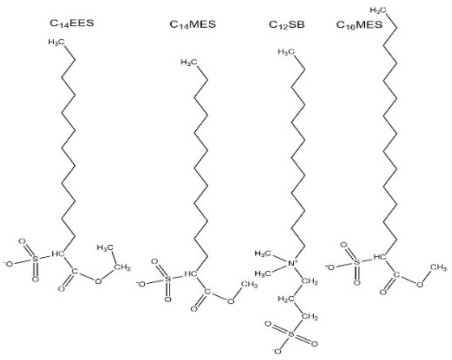

Figure 1. *Structure of C_{12}SB, C_{14}MES, C_{16}MES, and C_{14}EES surfactants.*

The molecules are drawn to represent their likely conformation at the interface, reflecting the need for the ester group to be in the hydrophobic region, and where the ester sulfonate group may sit with respect to the charges on the $C_{12}SB$.

The $C_{12}SB$ was prepared following the method of Qu et al (3) and described in detail for both the hydrogeneous and deuterated forms by Li et al (21). The surfactants were recrystallized from mixtures of acetone and methanol until no minimum in the ST was observed.

The synthesis and purification of $C_{14}MES$, $C_{16}MES$ and $C_{14}EES$ was as described by Wang et al (36) and Thomas et al (34). From ST and NMR the purity of these surfactants was at least > 99.5 %, as previously discussed (34, 36).

The solutions for the ST, NR and SANS measurements were made using Deuterium Oxide, D_2O, from Sigma Aldrich, high purity water (resistivity ~ 18.2 MΩcm), and analytic grade NaCl (>99.9% purity). All glassware associated with sample preparation, the quartz spectrophotometer cells for the SANS measurements, and the Teflon troughs for the NR studies, were all cleaned in alkali detergent (Decon90) and extensively rinsed in high purity water. All the measurements were made at 25±1°C, and no adjustments were made for pH, which was measured and was in the range 8.0 to 9.0.

(ii) Surface Tension

The surface tension measurements were made on a Kruss K11 maximum pull tensiometer using a platinum plate. The plate was rinsed in high purity water and dried between measurements. The tensiometer was calibrated for the ST of pure water, of 72 mNm^{-1}. Measurements were made by dilution from a concentration above the cmc, and each measurement was repeated until the variation in ST was ≤ 0.1 mN m^{-1}. The average value at each concentration was plotted, with an associated error ≤ 0.1 mN m^{-1}.

(iii) Neutron Reflectivity Instrumentation

The neutron reflectivity measurements were made on two separate reflectometers, the SURF reflectometer (37) on the ISIS neutron source, and the FIGARO reflectometer (38) at the Institute Laue Langevin. In both cases the reflectivity, R(Q), measurements were made at the air-water interface using the 'white beam time of flight' method to cover a wide range of Q values simultaneously. Q is the wave vector transfer perpendicular to the surface and is defined as $Q=4\pi\sin\theta/\lambda$, where θ is the grazing angle of incidence and λ the neutron wavelength. All the

measurements were made in null reflecting water, nrw, 8.1 % v/v D_2O / H_2O mixture with a scattering length density of zero and a refractive index of unity, and at 25±1°C.

On the reflectometer SURF (37) the measurements were made with θ=1.5° and neutron wavelengths in the range 1 to 7 Å to cover a Q range ~ 0.045 to 0.35 $Å^{-1}$, with a Q resolution ~ 5%. The reflectivity was normalised to an absolute scale by reference to the direct beam and the reflectivity from a known surface, D_2O, using the standard procedures for the instrument (37). The samples were contained in Teflon troughs with a sample volume ~ 25 ml, and measured sequentially on a 5 position sample changer. Each sample was measured for ~ 40 mins. The high Q limit of the data is determined by the point at which the background incoherent scattering from the aqueous subphase is comparable to the sample signal, and is not subtracted from the data before analysis.

The NR measurements on FIGARO (38) were made at a θ of 3.77° with a $\Delta\lambda/\lambda$ of 7% to provide a Q range of 0.03 to 0.3 $Å^{-1}$. The raw time of flight data were calibrated with respect to the incident wavelength distribution and detector efficiency using COSMOS (38) to produce a background subtracted and normalised R(Q). The measurement time for each sample was ~ 45 mins, using sequential measurements in 6 sealed Teflon troughs with sample volumes ~ 18 ml.

(iv) Small angle scattering instrumentation

The SANS measurements were made on the LOQ (39), SANS2D (40), LARMOR (41) and ZOOM (42) diffractometers at the ISIS neutron source, to obtain the scattered intensity, I(Q), as a function of the scattering vector Q, where Q is defined as $Q=4\pi\sin\theta/\lambda$ and 2θ is the scattering angle. On SANS2D a neutron wavelength range of 2 to 16.5 Å and a sample to detector distance of 4 m provided an accessible Q range of 0.006 to 0.8 $Å^{-1}$. On LOQ the equivalent Q range was from 0.008 to 0.25 $Å^{-1}$, from a sample to detector distance of 4.15 m and a wavelength range of 2 to 10 Å. The SANS measurements on LARMOR were made with a neutron wavelength range of 1 to 13 Å, to cover a nominal Q range of 0.003 to 0.7 $Å^{-1}$ (41). The SANS measurements on ZOOM were made using time-of-flight, to cover simultaneously a Q range of 0.0045 to 0.6 $Å^{-1}$ using an incident wavelength range of 1.75 to 16.5 Å and collimation settings for the incident and scattered flight paths of 4 m. The solutions were contained in quartz spectrophotometer cells with a path length of 2 mm and were maintained at a temperature of 25±1°C. The scattering from the empty cell and solvent was subtracted from the raw data and the data were normalised to the detector response, spectral distribution

of the incident neutron beam and the solid angle subtended by the detector to establish I(Q) on an absolute scale in cm^{-1} (43).

(b) Neutron Reflectivity

The neutron reflectivity measurements were made at the air-water interface for deuterium labelled surfactants in nrw. In these circumstances the reflectivity arises only from the adsorbed layer of deuterium labelled surfactant at the interface. For this situation it is well established (28) that the reflectivity can be described by a single thin layer of uniform composition and density, and is described by the exact equation,

$$R(Q) = \frac{16\pi^2}{Q^4}(2\rho)^2 \sin\left(\frac{Qd}{2}\right)^2 \qquad (1)$$

where d and ρ are the thickness and scattering length density of the adsorbed layer. As discussed in detail by Lu et al (28) the product d.ρ is then directly related to the adsorbed amount as described later in the paper.

(c) SANS

The SANS data for the mixed micelles are analysed quantitatively using the expression for the scattering from globular interacting micelles, which in the decoupling approximation, is written as (44),

$$I(Q) = n\left[S(Q)\left|\langle F(Q)\rangle_Q\right|^2 + \left\langle |F(Q)|^2 \right\rangle_Q - \left|\langle F(Q)\rangle_Q\right|^2 \right] \qquad (2)$$

where $< >_Q$ denotes averages over micelle size and orientation (where the decoupling approximation assumes no correlation in position, size, and orientation), n is the micelle number density, $S(Q)$ the structure factor describing the interactions between micelles. It is calculated using the rescaled mean spherical approximation for a repulsive screened Coulombic potential (45, 46), and is characterised by the micelle charge, z, the micelle diameter and concentration. $F(Q)$ is the form factor describing the micelle size and shape, and is modelled using the standard 'core-shell' micelle model (44).

It was previously shown that in the dilute and low Q limits the ratio of scattered intensities for the different isotopically labelled combinations in mixed micelle solutions can be used to determine the micelle composition (27). Assuming P(Q) = S(Q) =1.0, or at least that they are constant in shape with contrast then,

$$I(Q) = \sum_i N_i V_i^2 \left(\rho_{ip} - \rho_s\right)^2 \quad (3)$$

where V is the micelle 'dry' volume, ρ_p is the micelle scattering length density, ρ_s the solvent scattering length density, and the Σ_i is a summation over all the compositions. For a binary mixture, and for example for the two contrast combinations for C_{12}SB / C_{14}MES, hh/D_2O and hd/D_2O, then the volume fraction, V_f, is given by,

$$V_f = \left(\sqrt{R} - 1\right)(\rho_{hbet} - \rho_{D2O}) \Big/ (\rho_{hmes} - \rho_{hbet}) - \sqrt{R}(\rho_{dmes} - \rho_{hbet}) \quad (4)$$

and $\sqrt{R} = I_{hh}/I_{hd}$. From the known molecular volumes the mole fraction, M_f, can be straightforwardly calculated from the V_f.

(d) Pseudo Phase Approximation

The surface and micelle mixing properties are evaluated quantitatively using recent developments in the application of the pseudo phase approximation, PPA (21, 29-32). In the PPA the chemical potential of the different pseudo phases, surface, micelle and monomer, are assumed to be equal (47, 48). Equating, for example, the monomer and micelle chemical potentials gives,

$$x_i = C_i^{mon} / f_i^{\mu} C_i^{\mu} \quad (5)$$

where x_i is the mole fraction of the i^{th} component of the mixed micelle phase, C_i^{mon} the monomer concentration, f_i^{μ} the activity coefficient of the micelle and C_i^{μ} its cmc. For a binary mixture this gives rise to the expression for the mixed cmc,

$$\frac{1}{C_{mix}^{\mu}} = \frac{\alpha_1}{f_1 C_1^{\mu}} + \frac{\alpha_2}{f_2 C_2^{\mu}} \quad (6)$$

and for ideal mixing the activity coefficients are unity. The activity coefficients are determined by an expansion of the excess free energy of mixing, ΔGe, in a form that is consistent with the Gibbs Duhem equation (47, 48). Including quadratic, cubic and quartic terms (30-32) it can be expressed as,

$$\Delta Ge = x_1 x_2 B_{12} + x_1 x_2 (x_1 - x_2) C_{12} + x_1 x_2 (x_1 - x_2)^2 D_{12} \quad (7)$$

where B_{12}, C_{12}, and D_{12} are the interaction coefficients, and are here abbreviated to B, C, and D. In the RST approximation C and D are zero and the interaction is symmetrical with composition. C and D largely account for any asymmetry in the interaction and the detailed shape of the free energy curve.

Using this approach (27, 29-32) a set of equations which determine the variation in micelle composition, and the surface and monomer concentrations below and above the cmc can be defined. In the subsequent analysis of the mixing data presented here the interaction parameters are constrained to fit the cmc

variations and the surface and micelle composition variations, and provides a more rigorous evaluation of the thermodynamics of mixing (29). It was shown (29-31) that although the PPA is strictly applicable to nonionic mixtures, the higher order terms accommodate can charge interactions and so the asymmetry introduced accounts for the electrostatic interactions, packing requirements and changes in hydration. In particular it provides the opportunity to identify the steric and electrostatic contributions to the excess free energy of mixing, and the detailed shape of the free energy curve.

(e) Measurements made

The following measurements were made using the three different experimental techniques, ST, NR and SANS:

(i) Surface tension measurements were made for C_{12}SB / C_{14}MES, with and without 0.1 M NaCl, and for C_{12}SB / C_{16}MES.

(ii) NR measurements were made for the isotopic combinations of dd, dh, and hd in nrw for C_{12}SB / C_{14}MES with and without 0.1 M NaCl and for C_{12}SB / C_{16}MES, for concentrations from 0.1 to 5 mM and for solution compositions of 25/75, 50/50 and 75/25 mole ratio.

(iii) SANS measurements were made for the isotopic combinations of hh, dh, and hd in D_2O for C_{12}SB / C_{14}MES, with and without 0.1 M NaCl, in the concentration range 2 to 20 mM and for solution compositions of 25/75, 50/50 and 75/25 mole ratio. For 20 mM 50/50 C_{12}SB / SDS in D_2O measurements were made for the isotopic combinations of hh, dh, and hd. For C_{12}SB / C_{14}EES measurements were made for concentrations from 2 to 20 mM, solution compositions of 25/75, 50/50, and 75/25, for the isotopic combination of hh / D_2O only. Measurements were also made in D_2O and in 0.1 M NaCl for C_{12}SB, C_{14}MES and in D_2O for C_{14}EES.

RESULTS and DISCUSSION

(i) Surface Mixing at the air-water interface and in micelles

The nature of the surface and micelle mixing was determined using a combination of three different experimental approaches. The variation in the cmc was determined for C_{12}SB / C_{14}MES in the absence and presence of 0.1 M NaCl, and for C_{12}SB / C_{16}MES, using ST. The variation in the composition of the adsorbed layer at the air-water interface was determined by NR using the isotopic combinations of dd, dh and hd in nrw for C_{12}SB / C_{14}MES in the absence and presence of 0.1M NaCl, and for C_{12}SB / C_{16}MES. The micelle compositions were

determined using SANS and the isotopic combinations dh, and hd in D_2O for $C_{12}SB$ / $C_{14}MES$, and hh, hd in D_2O for $C_{12}SB$ / $C_{14}MES$ / 0.1 M NaCl.

Surface tension data for $C_{12}SB$ / $C_{14}MES$ are shown in figure S1 in the Supporting Information, and similar data were determined for $C_{12}SB$ / $C_{14}MES$ / 0.1 M NaCl and for $C_{12}SB$ / $C_{16}MES$, but are not shown.

The variation in the slopes of γ versus ln(C) below the cmc (the cmc is determined from the sharp break point in the data at surfactant concentrations ~ 0.5 to 2 mM) reflect the changing adsorption from pure $C_{12}SB$ and $C_{14}MES$ components to the mixture. The notable features are the significant reduction in the cmc and the ST at the cmc on mixing. The variation in the cmc with composition is more clearly seen in figure 2 and figure S2 in the Supporting Information; where the variation in cmc is plotted for all three mixtures measured, for the cmc values summarised in table S1 in the Supporting Information.

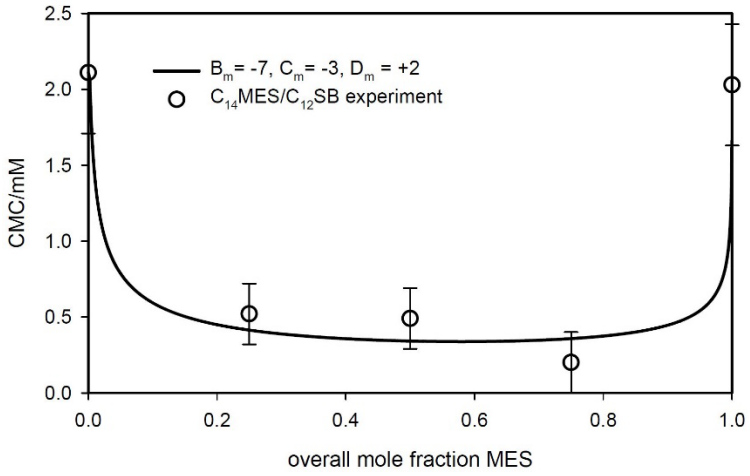

Figure 2. *Variation in cmc with solution composition for $C_{12}SB$ / $C_{14}MES$, from the data summarised in table S1 in the Supporting Information; see legend for details. The solid lines are PPA calculations as discussed later and for the parameters in table 2.*

The general trend observed is broadly similar for all the three surfactant mixtures. That is, on mixing the cmc is significantly reduced and is relatively constant with composition. The change observed in the cmc on mixing is indicative of a strong synergistic interaction between the zwitterionic and anionic surfactants, similar to that previously reported for $C_{12}SB$ / SDS (21). The solid lines in figures 2 and S2 in the Supporting Information are pseudo phase

approximation calculations, as described in detail in the section that follows and using the approach outlined in the Experimental Details and Methods section.

The fits in figures S2 a and b overestimate slightly the interaction. This is because the best fits for all the associated data for these mixtures, which include the surface and micelle compositions, also depend upon the cmc values. Hence the fits in figure S2 a and b correspond to the best overall fits for all the associated data.

NR measurements were made at the air-water interface to determine the amounts of the individual components in the different binary surfactant mixtures adsorbed at the interface. The measurements were made for deuterium labelled surfactants (see Experimental Details and Methods) in nrw. As described elsewhere (28), in these circumstances the measured reflectivity arises only from the adsorbed layer at the interface. Measurements were made for the isotopic combinations dd, dh and hd for C_{12}SB / C_{14}MES, C_{12}SB / C_{14}MES / 0.1 M NaCl and C_{12}SB / C_{16}MES. Some typical reflectivity data are shown in figure 3 for 5 mM 50/50 mole ratio C_{12}SB / C_{14}MES in nrw for the isotopic combinations of dd, dh, and hd.

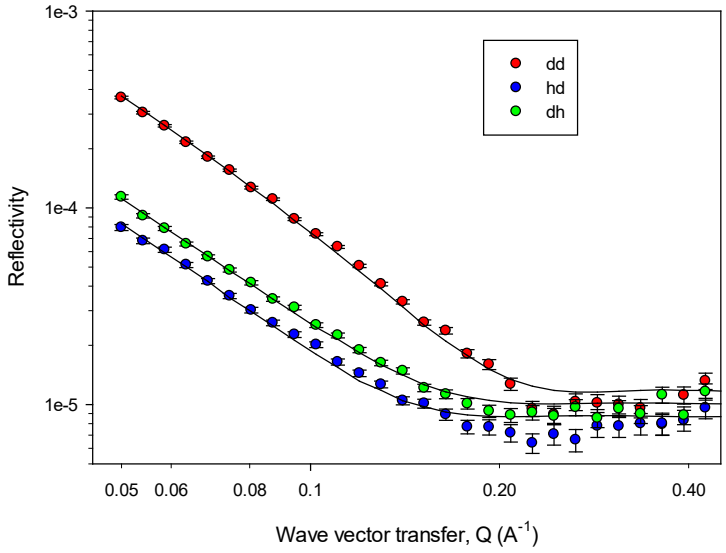

Figure 3. *Neutron reflectivity data (Reflectivity versus wave vector transfer, Q) for 5 mM 50/50* mole ratio C_{12}SB / C_{14}MES in nrw for the isotopic combinations of dd, dh, and hd (see legend *for details). The solid lines are model calculations as described in the main text and for the parameters summarised in table S2 in the Supporting Information.*

As described elsewhere (28) the data are well described by a single layer of uniform composition and density, and are analysed using equation 1 to obtain a thickness, d, and a

scattering length density, ρ. The product d.ρ is directly related to the adsorbed amount by d.ρ=Σb/A, where Σb is the sum of scattering lengths of labelled component at the interface and A is the area/molecule. The key model parameters for the data in figure 3 are summarised in table S2 in the Supporting Information.

The mean thickness of the adsorbed layer, averaged over all the data is ~ 22 ±3 Å, consistent with other studies (28) in similar circumstances. The measurements from the three different isotopic combinations result in three simultaneous equations of the form,

$$d\rho = \frac{\sum b_1}{A_1} + \frac{\sum b_2}{A_2} \qquad (8)$$

The three simultaneous equations are solved by least squares, using the Σb values in table S3 in the Supporting Information, to obtain the area / molecule, A, (and adsorbed amount, Γ, where Γ=1/NaA, and Na is Avogadro's number) of each component, the total adsorbed amount, and the surface composition.

The derived adsorption and composition data for the three surfactant combinations measured are summarised in tables 1 and S4 and S5 in the Supporting Information, where the data were determined for three solution compositions, 25/75, 50/50 and 75/25 mole ratios, and for a range of surfactant concentrations from below to in excess of the mixture cmc.

Table 1. *Adsorption parameters for $C_{12}SB$ / $C_{14}MES$*

Conc. (mM)	**Composition ($C_{12}SB$/$C_{14}MES$)**	**A ($C_{12}SB$) (Å^2)**	**Γ ($C_{12}SB$) (x10^{-10} mol cm^{-2})**	**A ($C_{14}MES$)**	**Γ($C_{14}MES$)**	**Γ(total)**	**Mole fraction $C_{12}SB$**
0.1	0.25	81	2.05	140	1.19	3.24	0.63
0.25		78	2.13	78	2.13	4.26	0.50
0.5		71	2.34	70	2.37	4.71	0.50
1.0		69	2.41	65	2.55	4.96	0.49
2.0		76	2.18	65	2.55	4.73	0.46
5.0		92	1.80	66	2.52	4.32	0.42
0.1	0.5	73	2.27	139	1.19	3.46	0.66
0.25		72	2.31	89	1.87	4.18	0.55
0.5		67	2.48	83	2.00	4.48	0.55
1.0		61	2.72	79	2.10	4.82	0.56
2.0		62	2.68	83	2.00	4.68	0.57
5.0		63	2.63	75	2.21	4.84	0.54

0.1	0.75	74	2.24	134	1.24	3.48	0.64
0.25		58	2.86	139	1.19	4.05	0.71
0.5		61	2.72	92	1.80	4.52	0.60
1.0		59	2.81	100	1.66	4.47	0.63
2.0		57	2.91	111	1.50	4.41	0.66
5.0		65	2.55	88	1.89	4.44	0.57

The adsorption for the pure C_{12}SB, C_{14}MES, and C_{16}MES, at a concentration > cmc, have been previously determined (21, 34-36) and are summarised in table S6 in the Supporting Information.

The general trends in the adsorption for the C_{12}SB / C_{14}MES mixture are illustrated in figure 4, and S3 in the Supporting Information broadly similar trends are observed for the other mixtures measured.

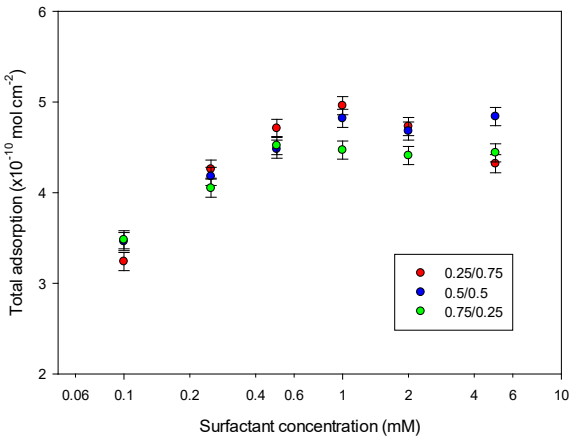

(a)

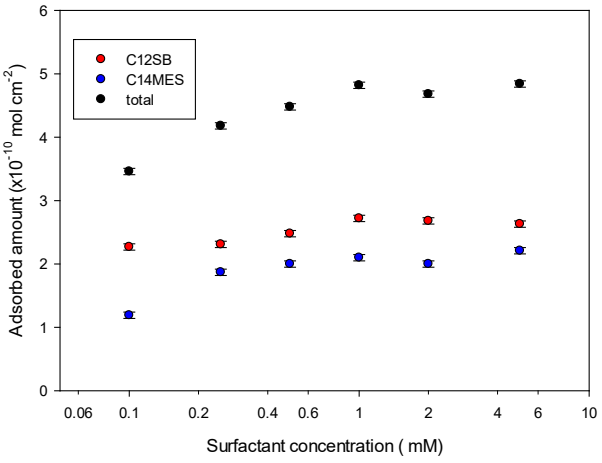

(b)

Figure 4. *Adsorption data for C_{12}SB / C_{14}MES, (a) Total adsorption versus concentration for 75/25, 50/50 and 25/75 mole ratio solution compositions and (b) variation in total adsorption and amounts of C_{12}SB and C_{14}MES with concentration for 50/50, see legend for details.*

For all three surfactant mixtures the adsorbed amount increases with increasing surfactant concentration and above the cmc reaches a plateau, broadly consistent with the Langmuir isotherm form. The mean adsorption for concentrations > cmc is within error constant with composition, as summarised in table S7 in the Supporting Information.

The notable exception is the data for 75/25 C_{12}SB / C_{14}MES. The data for C_{12}SB / C_{14}MES in 0.1 M NaCl is significantly higher than in the absence of electrolyte. The values for C_{12}SB / C_{16}MES are also systematically lower than those for C_{12}SB / C_{14}MES. The mean adsorption values in table S7 in the Supporting Information, when compared to the saturation adsorption values for the individual component surfactants, also imply a significant synergistic increase in the total adsorption on mixing, as previously demonstrated by Li et al (21) for C_{12}SB / SDS mixtures.

As shown in figure 4 and figure S3b in the Supporting Information, the variation in surface composition with concentration is relatively modest, and this is more clearly illustrated in figure 5 for all three mixtures.

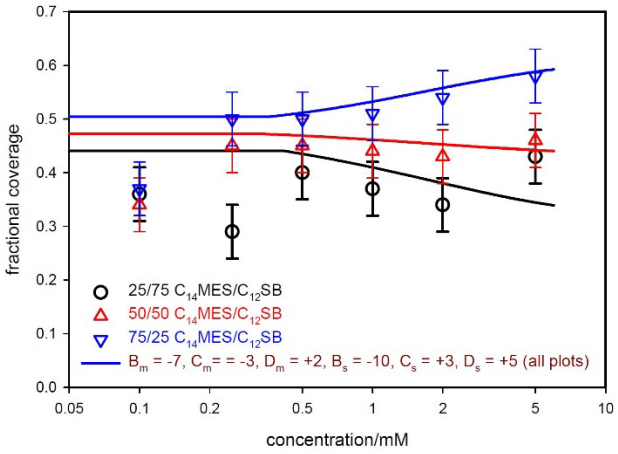

(a)

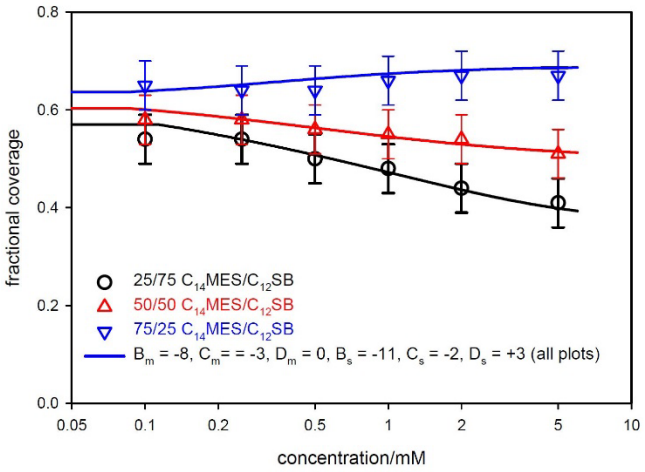

(b)

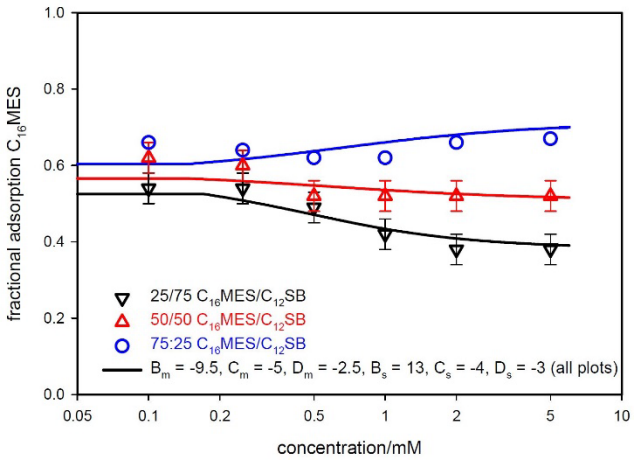

(c)

Figure 5. *Variation in surface composition (expressed as fractional coverage or fractional composition of C_{14}MES or C_{16}MES) with surfactant concentration for (a) C_{12}SB / C_{14}MES, (b) C_{12}SB / C_{14}MES / 0.1 M NaCl, and (c) C_{12}SB / C_{16}MES, see legends for details. The solid lines are PPA calculations for the parameters summarised in table 2.*

Table 2. *Pseudo phase approximation parameters from analysis of cmc variation, surface and micelle compositions for the C_{12}SB / alkyl ester sulfonate, AES, mixtures.*

(a) C_{12}SB / SDS (reproduced from reference 21)

	B	C	D	x_{sds}	ΔGe (RT)
Surface	-10.2	7.5	2.5	0.38	-2.8
Micelle	-5.0	8.5	-10.0	0.23	-2.2

(b) C_{12}SB / C_{14}MES

		B	C	D	x_{mes}	ΔGe (RT)
No salt	**Surface**	-10.0	3.0	5.0	0.45	-2.54
	Micelle	-7.0	-3.0	2.0	0.58	-1.81
0.1M NaCl	**Surface**	-11.0	-2.0	3.0	0.54	-2.76
	Micelle	-8.0	-3.0	-	0.59	-2.07

(c) C_{12}SB / C_{16}MES

	B	C	D	x_{sds}	ΔGe (RT)
Surface	-13.0	-4.0	-3.0	0.59	-3.34
Micelle (cmc only)	-8.5	-5.0	-2.5	0.65	-2.33

The relatively small change in the surface composition with concentration, for concentrations above the cmc, is associated with the relatively modest variation in the cmc over the range of compositions measured. This was previously demonstrated in some anionic / nonionic surfactant mixtures using RST by Staples et al (49), and is a key feature of such mixing behaviours. Furthermore, although the surface compositions tend towards the solution composition as the concentration increases they are still significantly different to the solution composition at the highest concentrations measured. In the PPA (26, 46, 47), as will be discussed in more detail in a later section of the paper, although the micelle composition must tend towards the solution composition with increasing concentration, the surface can adopt a different composition as it is controlled primarily by the monomer composition and concentration. The other main feature is that below the cmc the variation in the surface composition with concentration should be constant, and this is clearly observed for C_{12}SB / C_{14}MES / 0.1 M NaCl and for C_{12}SB / C_{16}MES (see figures 5 b and c), and is consistent with previous observations on related mixtures (50). The equivalent data for C_{12}SB / C_{14}MES (see figure 5a) in the region below the cmc just reflects a greater uncertainty in that particular data.

The micelle compositions for C_{12}SB / C_{14}MES, with and without 0.1 M NaCl, were determined using SANS with different isotopically labelled surfactants in D_2O; for C_{12}SB / C_{14}MES using dh and hd, and for C_{12}SB / C_{14}MES / 0.1 M NaCl using hh and hd. Using known scattering length densities (see table S8 in the Supporting Information), and molecular volumes, the ratio of the scattered intensities extrapolated to low Q are related to the micelle composition, expressed either as a volume or mole fraction, using equations 3 and 4.

The variation in micelle composition for C_{12}SB / C_{14}MES, in the absence and presence of 0.1 M NaCl, for the three different solution compositions, 25/75, 50/50, and 75/25 mole ratio and for concentrations from 2 to 20 mM are shown in figure 6, and summarised in table S9 in the Supporting Information.

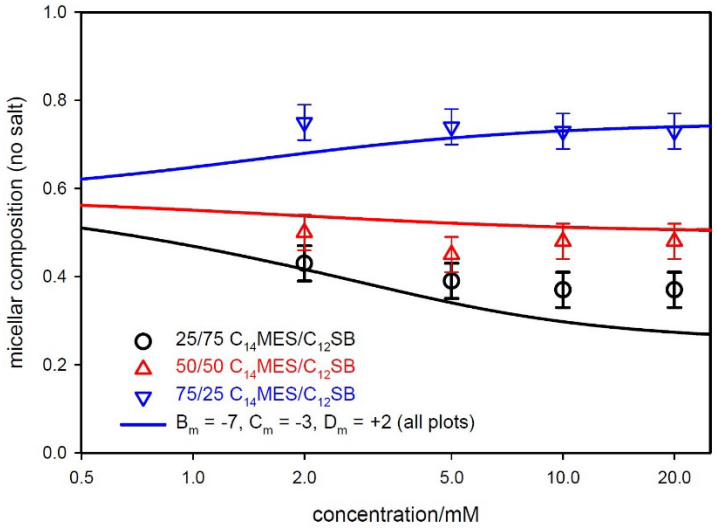

(a)

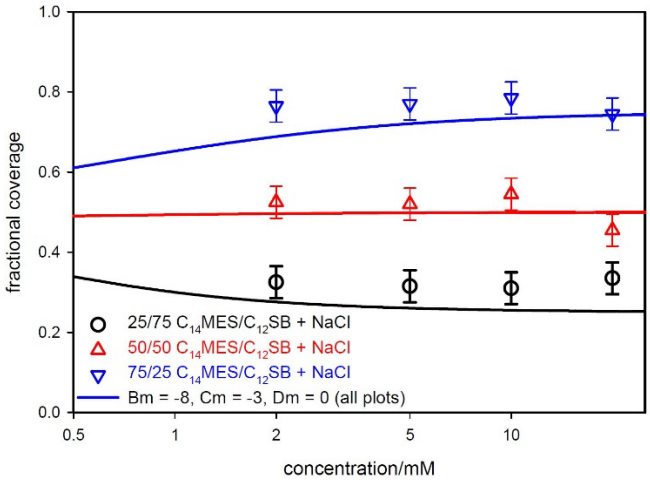

(b)

Figure 6. *Variation in micelle composition (expressed as micelle composition of fractional coverage of C_{14}MES) with surfactant concentration for (a) C_{12}SB / C_{14}MES in D_2O and (b) C_{12}SB / C_{14}MES / 0.1 M NaCl in D_2O, see legends for details. The solid lines are PPA calculations for the parameters summarised in table 2.*

A detailed evaluation and discussion of the SANS data with respect to the micelle structure will be presented in a later section. However, similar to the variation in the surface composition with concentration and for broadly similar reasons, the micelle composition varies only slightly with concentration. Furthermore, given the relatively large errors in the determination of the composition, the composition is essentially constant over the concentration and compositions ranges measured. The notable difference, compared to the surface composition, is that the micelle composition is now similar to the solution composition, as would be expected from the previous discussions.

(ii) Thermodynamics of mixing

In mixed systems, the combination of cmc data, surface compositions from NR, and micelle compositions from SANS allows a more precise characterisation of the surfactant interaction (21, 29, 31). In particular it provides the opportunity to apply the PPA with an expansion of the excess free energy of mixing, ΔG_e, which goes beyond the symmetrical RST approach (47, 48). It enables the inclusion of quartic and cubic terms in addition to the RST quadratic term, in way consistent with the Gibbs-Duhem equation, as described earlier.

Hence the approach here is similar to that outlined recently for C_{12}SB / SDS (21) and for some ternary mixtures (30, 31), where a consistent set of micelle and surface interaction parameters are determined to obtain the best description of the cmc, micelle and surface composition data. The key interaction parameters derived from the analysis are summarised in table 2, and for the surface and micelle mixing all the mixtures studied required quadratic, cubic and quartic terms in the expansion of ΔG_e, see equation 7. The corresponding excess free energy curves are shown in figure 7, and the corresponding values of the excess free energy minimum and the composition at the minimum are included in table 2.

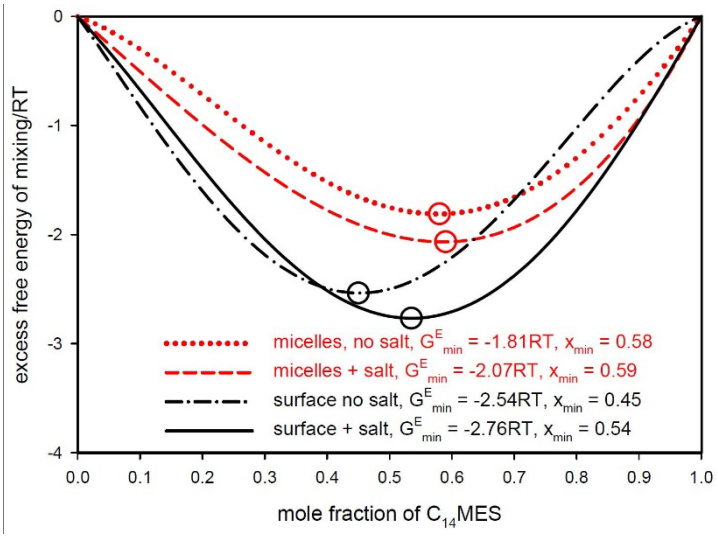

(a)

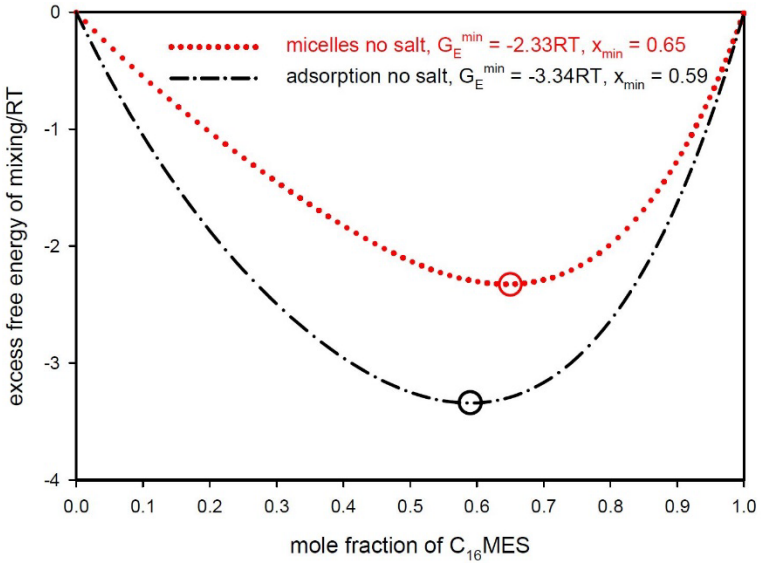

(b)

Figure 7. *Excess free energy of mixing versus composition for (a) C_{12}SB / C_{14}MES, (b) C_{12}SB / C_{16}MES, see legend for details*

The parameters in table 2 show that for C_{12}SB / C_{14}MES, with and without salt, and for C_{12}SB / C_{16}MES, a strong attractive synergistic interaction exists, and that it is broadly similar to that previously reported for C_{12}SB / SDS (21). An attractive synergistic interaction is not unexpected, and was reported recently, for example, in nonionic / anionic mixtures due to a reduction in the repulsive interactions (29-32). However the excess free energy values reported in table 2 are significantly greater than for the range of nonionic / anionic systems recently investigated (29-32) using a similar approach. Li et al (21) discussed this in the context of C_{12}SB / SDS mixtures. There the C_{12}SB is electrically neutral, but contains separate positive

and negative charges, and although the C_{12}SB acts in principle as a nonionic surfactant the charge separation introduces additional factors. This will be explored further in this section.

The interaction parameters in table 2 also show consistently for these mixtures that the surface interaction is stronger than the micelle interaction, resulting in a larger excess free energy of mixing at the surface than in the micelles. This was also observed by Li et al (21) for C_{12}SB / SDS mixtures, and in a range of nonionic / anionic surfactant mixtures (29-31). The difference is associated with a more relaxed packing constraint and ability to minimise headgroup interaction in the micelle geometry than at a planar surface or interface.

As described earlier the finite values of the higher order terms in the expansion of excess free energy of mixing in table 2, the cubic and quartic terms in addition to the quadratic term, indicate that for all the mixtures the interaction is asymmetrical with respect to the composition, and is not consistent with a symmetrical RST description. The relative values of the interaction parameters C and D also determine the shape of the excess free energy curve. The variations in the excess free energy curves for the different mixtures and for the surface compared to the micelle mixing are shown in figure 7.

For the mixture C_{12}SB / C_{14}MES measurements were made with and without added electrolyte, in order to gain more insight into the strength and nature of the electrostatic interaction. This was specifically explored by Liley et al (30, 31) for the binary and ternary mixtures of sodium diethylene glycol monododecyl ether sulfate, SLES, sodium dodedecyl 6-benzene sulfonate, LAS and $C_{12}E_8$. In that case the addition of 0.1 M NaCl weakened the SLES-$C_{12}E_8$ and the LAS-$C_{12}E_8$ interactions, consistent with them being dominated by electrostatic interactions. However the SLES –LAS interaction was hardly affected by electrolyte, which implied that the interaction is largely attributable to structural / packing considerations. For C_{12}SB / C_{14}MES the strength of the interaction increases slightly with the addition of electrolyte. This implies that although the addition of electrolyte will reduce the impact of electrostatic interactions it is offset by an enhanced interaction due to packing considerations, structural alterations or hydrophobic interactions. The ΔGe values for the surface for C_{12}SB / C_{16}MES mixture is larger than for the other mixtures, and this implies a greater packing or hydrophobic contribution to the interaction associated with the longer alkyl chain length of the C_{16}MES.

The other notable feature in table 2 and figure 7 is the surface and micelle compositions corresponding to the excess free energy minimum. Firstly the values for C_{12}SB / C_{14}MES, with and without salt, and for C_{12}SB / C_{16}MES are quite different to those for C_{12}SB / SDS. The

values for C_{12}SB / SDS imply a much greater asymmetry than for the MES containing mixtures. For the C_{12}SB / MES mixtures, apart from the surface mixing for C_{12}SB / C_{14}MES in the absence of salt where the composition corresponding to the minimum in ΔGe is roughly equimolar, the composition corresponding to the ΔGe minimum is MES rich and ~ 058±0.02 mole fraction MES. At the surface in an ordered 2D mixture of charged and uncharged species the simplest hexagonal lattice arrangement for minimising the electrostatic repulsion is 2:1 nonionic / ionic. This was what was largely reported by Liley et al (30) for $C_{12}E_8$ / SLES and $C_{12}E_8$ / LAS mixtures. Patist et al (51) observed an enhancement in surface properties for a mole fraction of 0.3 SDS in nonionic / SDS mixtures. Reif and Somasundaran (52) reported a minimum in the excess free energy at a similar composition. However in their analysis this was associated with a variable interaction parameter, B, using the RST approach, and which is incompatible with the Gibbs-Dunhem requirement of the PPA. However the values reported in this study imply a significant packing, structural or hydrophobic contribution to the interaction.

The strong synergistic interaction between C_{12}SB and the anionic cosurfactants, when comparing the values of saturation adsorption of the individual components in table S6 in the Supporting Information with the mean saturation values for the three different mixtures in table S7 in the Supporting Information, results in a strong enhancement in the total adsorption on mixing. The relative increase in the total adsorption for C_{12}SB / C_{14}MES is ~ 35%, for C_{12}SB / C_{14}MES / 0.1 M NaCl ~47% and for C_{12}SB / C_{16}MES ~ 21%. This compares with an increase ~ 58% for C_{12}SB / SDS (21). Such relatively large increases are not always observed, and were recently discussed by Liley et al (32) in the context of 5-component surfactant mixtures composed of anionic, nonionic surfactants and rhamnolipids. Furthermore in nonionic / anionic surfactant mixtures in the presence of electrolyte (29, 49), where the interaction is less pronounced, significant enhancements in the total adsorption are not generally observed. Li et al (21) discussed in detail the origins of the enhanced adsorption on mixing and its associated reduction in the free energy for C_{12}SB / SDS mixtures. The tighter packing was attributed to a rearrangement of the zwitterion. It is assumed that the interaction with the anionic surfactant results in the zwitterion headgroup being more fully extended, resulting in tighter packing. Whereas an isolated C_{12}SB molecule would adopt a configuration for the trimethylene chain separating the two charged groups which would allow a closer proximity for the two charged groups. This would inevitably result in a more bulky headgroup arrangement. Consistent with that argument, the reduced enhancement in the adsorption for the C_{12}SB / C_{14}MES mixture is associated with the bulkier methyl ester headgroup of C_{14}MES compared to the sulfate group

of SDS resulting in a less efficient packing with the zwitterion and a reduce rearrangement of the zwitterion.

Although for C_{12}SB / C_{14}MES the addition of electrolyte does not substantially change the excess free energy of mixing, the enhancement in the total adsorption does increase further compared to the absence of electrolyte. This implies that the improved packing arising from the addition of electrolyte does not significantly increase the strength of the synergistic interaction. However the excess free energy of mixing does increase slightly, from -2.54 to -2.76 RT, and this change is then associated with the improved packing observed.

The enhancement in the adsorption for the C_{12}SB / C_{16}MES mixture is noticeably reduced, ~ 25%, and this implies that the mismatch in alkyl chain length for the C_{16}MES results in a less efficient packing at the interface.

The main features of the strong synergistic interaction between C_{12}SB and the different anionic surfactants studied are: (a) pronounced asymmetry which occurs at C_{12}SB rich compositions for C_{12S}B / SDS mixtures and at MES rich compositions for C_{12}SB / C_{14}MES mixtures, (b) modest increase in the excess free energy of mixing with the addition of 0.1 M NaCl, (c) pronounced enhancement in the total adsorption on mixing and the extent of the enhancement for the different anionic surfactants. Although there is a strong electrostatic component to the interaction these trends indicate a significant contribution due to packing considerations and structural alterations. Indeed following the arguments of Li et al (21) the rearrangement of the zwitterion due to the presence of the anionic headgroup is the major factor. Changing the headgroup structure from sulfate to the bulkier methyl ester reduces the structural change. Furthermore changes from C_{14}MES to C_{16}MES introduces an additional hydrophobic contribution to the interaction.

Finally the excess free energy values on mixing are reduced for micellisation compared to the surface mixing. This implies that the packing constraint in micelles are less severe than at the surface. However, they will have a significant impact on the micellisation, and this is discussed in detail in the following section.

(iii) Micelle Structure on mixing

A series of SANS measurements were made in order to characterise the nature of the mixed micelles. Most of the measurements were made for a combination of differently isotopically labelled surfactants in D_2O, and also for the pure component surfactants in D_2O. The

measurements for C_{12}SB / SDS were made in D_2O and in 0.1 M NaCl at a surfactant concentration of 20 mM, at an equimolar solution composition, and for the isotopic combinations of hh, hd and dh. The same isotopic combinations were used for C_{12}SB / C_{14}MES in D_2O and in 0.1 M NaCl, at surfactant concentrations of 5, 10 and 20 mM, and for solution compositions of 25/75, 50/50, and 75/25 mole ratio. Measurements for the C_{12}SB / C_{14}EES mixtures were made in D_2O and in 0.1 M NaCl at surfactant concentrations of 2, 5, 10 and 20 mM, for solution compositions of 25/75, 50/50 and 75/25, and only for the isotopic combination of hh in D_2O. Measurements were also made for the pure C_{12}SB, C_{14}MES and C_{14}EES components in D_2O and 0.1M NaCl at concentrations of 2, 5, 10 and 20 mM.

The SANS data are analysed quantitatively using the established model for the scattering from globular interacting micelles (44) as outlined in the Experimental Details. A constrained 'core-shell' model is used to describe the micelle size and shape (44) via the form factor F(Q). The micelle is modelled with an inner core, radius R1, containing the surfactant alkyl chains and constrained to have a maximum radius equal to the fully extended alkyl chain length, lc. An outer shell, radius R2, then space fills to contain the surfactant headgroups and associated hydration. For micelle aggregation numbers, ν, greater than can be accommodated in a spherical geometry, it is assumed that the micelle elongates as a prolate ellipsoid, with an elliptical ratio of ee. An additional parameter, ext, allows for fluctuations in the inner core constraint, such that R1=lc.ext. Using known molecular dimensions and neutron scattering lengths (see table S10 in the Supporting Information) the scattering is calculated on an absolute scale and compared by least squares with the data. The key model parameters are then ν and ext, and the inter-micellar interactions are determined by z, κ, and the micelle diameter and concentration. In the concentration range studied the micelle composition is assumed to be close to the solution composition, and is included in the calculation. In the calculations presented the model agrees mostly with the absolute scattering to within ±0.2, and the form of the scattering is well reproduced by the model.

The most extensive range of SANS data obtained was for the C_{12}SB / C_{14}MES mixture, with and without 0.1 M NaCl. A limited set of data for C_{12}SB / SDS were obtained to complement the surface data extensively discussed in reference 21. This data and some limited data for the C_{12}SB / C_{14}EES mixture also provide important additional insights which are important to interpret fully the trends observed for the C_{12}SB / C_{14}MES mixture.

Figure 8 shows the SANS data for 20 mM C_{12}SB / C_{14}MES in D_2O, for three different solution compositions, 25/75, 50/50 and 75/25 mole ratio, and for the different isotopic combinations, hh, dh, and hd in D_2O.

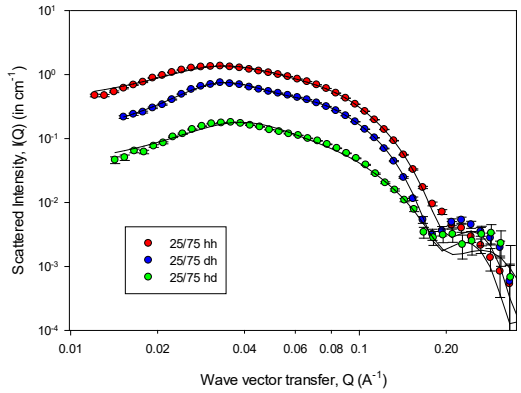

(a)

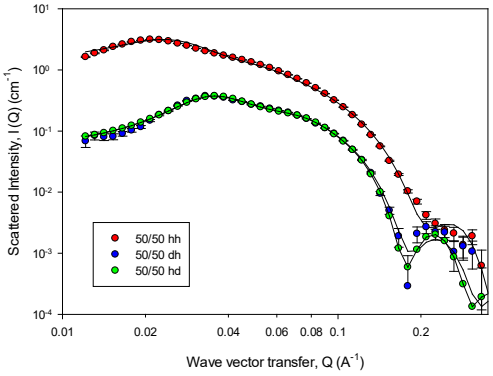

(b)

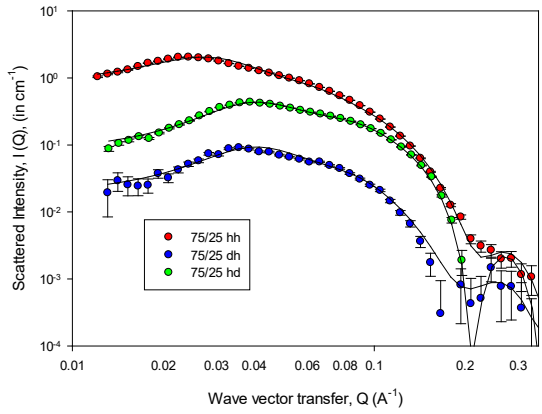

(c)

Figure 8. *SANS data for 20 mM C_{12}SB / C_{14}MES in D_2O for the isotopic combinations of hh, hd, and dh (see legend for details), (a) 25/75 mole ratio, (b) 50/50 and (c) 75/25. The solid lines are model calculations as described in the main text and for the key model parameters summarised in table S11a.*

The data are consistent with globular interacting micelles, and the key model parameters are summarised in table S11a using the model described earlier.

Broadly similar data are obtained at surfactant concentration of 5 and 10 mM, and although the data are not shown the key model parameters are also summarised in table S11a in the Supporting Information. The model provides mostly an adequate description of the data, and

certainly quantifies well the main features and trends. However the data for the different contrasts measured are analysed separately and illustrate a significant variation in the model parameters and hence in the micelle size. This is also clearly evident in the form of the data, where the interaction peak occurs at different Q values for the different contrasts. This indicates quite clearly, as confirmed by the detailed analysis, that the micelle number density and hence aggregation number is different for the different contrasts. This is not a situation normally encountered in other mixed systems (49, 57), and is associated with the strong synergistic interaction encountered for this mixture. However the variation is much less pronounced for the dh and hd isotopic combinations compared to hh combination. It was for this reason that the combination of the data for dh and hd were used to estimate the micelle compositions, as described in an earlier section. The variations with contrast imply an isotope effect and this is discussed again detail later in this section. The possibility of a different micelle structure was considered, but the form of the data strongly implies that the globular interacting micelles exist across the range of contrasts. The possibility of spatial separation within the micelle or the coexistence of micelles with different compositions were considered. It was not possible to convincingly reproduce the data trends using those assumptions, and the thermodynamic parameters also do not indicate such trends. Hence, apart from the data for hh / D_2O, the data and analysis do not suggest any strong trends with composition of concentration, and the aggregation number is ~ 80 to 120 and the degree of ionisation, δ (where $\delta=z/\nu$), is ~ 0.3.

To augment previous data (36) and for direct comparison SANS measurements were also made for C_{12}SB, C_{14}MES and C_{14}EES in the absence and presence of 0.1 M NaCl. The data, not shown here, are consistent with small globular interacting micelles and the key model parameters are summarised in table S12 in the Supporting Information.

The scattering from the C_{12}SB indicate no net charge and an aggregation number ~ 80. The equivalent C_{14}MES micelles have an aggregation number ~ 70 and a degree of ionisation ~ 0.3. In neither system is there any significant variation with concentration over the concentration range measured. The parameters for C_{14}MES and C_{14}EES are consistent with previous measurements (36), with those of other anionic surfactants in a similar concentration range, and notably with SDS (44, 53, 54). Comparison of these data with the data for C_{12}SB / C_{14}MES mixtures and for the contrasts dh and hd indicate some modest micelle growth on mixing.

The data shown in figure 9 is the equivalent data to that in figure 8, but in the presence of 0.1 M NaCl. The associated key model parameters are summarised in table S11b.

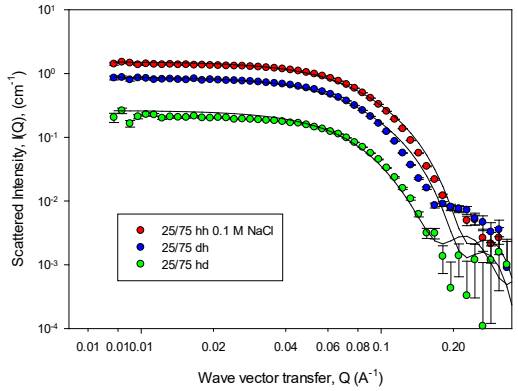

(a)

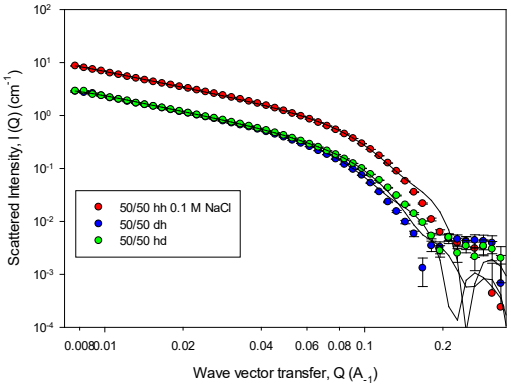

(b)

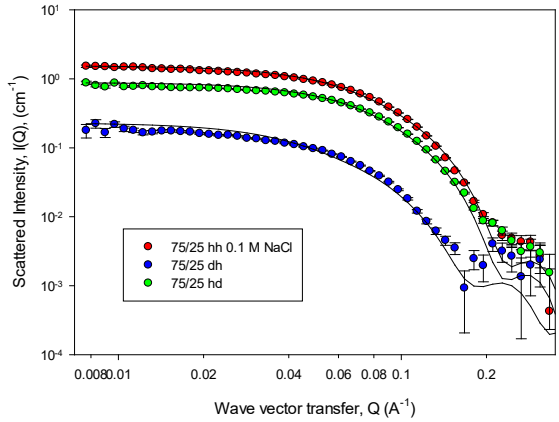

(c)

Figure 9. *As for figure 8, but in 01.M NaCl, and for the key model parameters in table S11b in the Supporting Information.*

The addition of 0.1M NaCl results in a different form to the SANS data. For the solution compositions 25/75 and 75/25, see figures 9 a and c, the data are still consistent with globular micelles with a relatively modest size and aggregation number. But the addition of electrolyte has screened the inter-micellar interactions and the form of the scattering reflects mainly the micelle form factor, F(Q), which is consistent with globular micelles, and the core-shell model does still replicates the data well. At those two solution compositions the value for the

aggregation number, ~150, indicates some modest growth which is broadly independent of concentration. Furthermore the variations in the model parameters across the three different contrasts measured, hh, dh and hd, are in much closer correspondence, and are consistent with a single model being sufficient to describe the data. Comparing the aggregation numbers for the 25/75 and 75/25 compositions with the pure components in 0.1 M NaCl (see table S12b in the Supporting Information) shows that the mixing is promoting a synergistic increase in the micelle size. The data for the equimolar composition (see figure 9b) is quite different and the increased slope in the data at low Q values towards a Q^{-1} dependence is indicative of significant micellar growth. This is supported by the quantitative analysis which indicates a micelle aggregation number in the range 1000 to 2000. There is now also a greater range in the model parameters for the different contrasts than was observed for the other solution compositions in 0.1 M NaCl. This greater variation is not unexpected as the quantitative interpretation of the scattering data from such elongated structures is very sensitive to the Q range explored and to the accuracy of the data points in the low Q region. However the important observations are that in the presence of electrolyte the mixing results in a synergistic enhancement in the micelle growth, and that the growth is significantly more pronounced at the equimolar solution composition. These are particularly important observations as pronounced synergistic effects on micelle size are not usually observed in other nonionic / ionic surfactant mixtures (49, 55-57).

The sensitivity of the micelle growth to the addition of electrolyte and the solution composition also in part explains the variability with isotopic content for the data in the absence of electrolyte. If due to the synergistic interactions on mixing the mixed micelles are at the transition from relatively modestly sized globular micelles to more significantly elongated structures, then small variations such as a different isotopic composition may be sufficient to shift the transition point.

To augment the previously reported surface data for C_{12}SB / SDS mixtures (21) and to set the C_{12}SB / C_{14}MES SANS data in a wider context, some limited SANS measurements were made for 20 mM 50 /50 mole ratio C_{12}SB / SDS in the absence and presence of 0.1 M NaCl. The data are shown in figure S4 in the Supporting Information and the key model parameters are summarised in table S11 e and f in the Supporting Information.

The data in the absence of electrolyte (figure S4a in the Supporting Information) are consistent with small globular interacting micelles, with a similar structure for all three contrasts

measured, hh, dh and hd. The key model parameters in table S11e in the Supporting Information are now consistent for all the three contrasts measured. The aggregation number is ~ 150 and the degree of ionisation is ~ 0.1. Compared to the C_{12}SB / C_{14}MES mixtures the enhancement in the micelle size on mixing is larger and the charge on the micelle is lower. This is entirely consistent with the arguments presented in the discussion of the thermodynamics of mixing, where the SDS interacts more effectively with the zwitterion to induce improved packing and a degree of charge cancellation. Although it is assumed that the constraints are less severe in the micelles than at the surface, the impact is nevertheless evident.

In the presence of 0.1 M NaCl the equimolar mixtures of C_{12}SB / SBS undergoes significant micellar growth, and the data in figure S4b in the Supporting Information and table S11f in the Supporting Information are consistent with highly elongated micellar structures. Indeed the enhancement in the micelle aggregation is similar to that reported here for 50/ 50 C_{12}SB / C_{14}MES in 0.1 M NaCl, and the same considerations about the variations in the model parameters apply.

The similarity in behaviour for the equimolar C_{12}SB / C_{14}MES and C_{12}SB / SDS mixtures in 0.1 M NaCl imply that the improved packing of the zwitterion due to the presence of the anionic headgroup (as discussed earlier) and the additional suppression of electrostatic interactions by the addition of electrolyte improves the micelle packing sufficiently to promote significant micellar growth. However it is surprising that the onset of growth is so sensitive to the solution composition.

Finally to further investigate the impact of the change in the anionic surfactant headgroup on the aggregation process, some additional measurements were made for the C_{12}SB / C_{14}EES mixture in D_2O and in 0.1 M NaCl. In this case the anionic headgroup is increased from methyl ester to ethyl ester Also in this case the measurements were limited to a range of surfactant concentrations, 2, 5, 10 and 20 mM and for a single isotopic combination, hh. The SANS data in the absence and presence of 0.1 M NaCl are shown in figure S5 and S6 in the Supporting Information.

At all the concentrations the data are well described by the same core-shell model for interacting globular micelles, and the key model parameters are summarised in tables S1 c and d in the Supporting Information. In the absence of electrolyte the scattering is consistent with micelles with some modest growth compared to the pure component micelles. The aggregation number is roughly constant with concentration and larger for C_{12}SB rich compositions.

However the micelle growth is not as pronounced as for the addition of C_{14}MES or SDS. Hence it is clear that compared to the C_{12}SB / C_{14}MES and C_{12}SB / SDS mixtures that the larger ethyl ester group is less effective at improving micelle packing than the sulfate or methyl ester groups.

The addition of electrolyte (see figure S6 and table S11d in the Supporting Information) results in significant micellar growth, just as was observed at an equimolar solution composition for C_{12}SB / SDS and C_{12}SB / C_{14}MES. Although the growth is again most significant for the equimolar solution composition and comparable to that observed for the other two mixtures, the growth observed at the other two solution compositions, 25/75 and 75/25 is more pronounced than for C_{12}SB / C_{14}MES. From previous measurements (36) C_{14}EES alone shows only modest growth in the presence of NaCl. Hence the growth observed here implies that the electrolyte is more effective at screening interactions in the C_{12}SB and C_{14}EES mixture than with SDS or C_{14}MES. Although there is no discernible trend with concentration at the equimolar composition, at 75 / 25 mole ratio the micelle growth increases with significantly with decreasing concentration, and for the 25/75 mole ratio the micelle growth increases with increasing concentration. This latter trend is consistent with expectations, but the former trend is counterintuitive. However a similar trend was reported by Chen et al (54) due to the impact of diamines on the self-assembly of SDS. This was in part attributed to the micellar growth at higher concentrations being limited by nearest neighbour interactions, whereas the impact of crowding is less significant at lower concentrations. However the difference in the trends with concentration for the compositions 25/75 and 75/25 indicate that the process is also affected by other factors.

The mixing of C_{14}MES, C_{14}EES and SDS with C_{12}SB all result in micellar growth, consistent with the synergistic interaction that results in the surface adsorption properties and in particular the enhanced adsorption. It was shown in the thermodynamic analysis using the PPA that in the C_{12}SB / SDS and C_{12}SB / C_{14}MES mixtures the interaction was stronger at the surface than in the micelles. This was attributed to the more severe packing constraints at the surface than in micelles. Nevertheless the interaction in the micelles is still significant and does drive the micelle growth on mixing. With the addition of electrolyte the micelle growth is more significant and strongly dependent upon the solution composition, As such it shows the most significant growth at an equimolar composition for all 3 mixtures. The trends without / with 0.1 M NaCl imply that in the absence of electrolyte the main factor contributing to the micelle growth is the improved packing, as discussed earlier. Although there is also an electrostatic

contribution in the absence of electrolyte, in 0.1 M NaCl it is the further reduction in the electrostatic interaction which dominates.

SUMMARY

The use of ST, NR and SANS to probe the interaction between C_{12}SB and a range of anionic surfactants extends the previously reported study by Li et al (21) on C_{12}SB / SDS mixtures. It also provided the opportunity for a more detailed thermodynamic analysis of the interaction in the mixtures at the surface and in micelles using recent developments in the PPA approach (21, 22, 29-31). As such it enabled a detailed evaluation which goes beyond that previously reported in some zwitterionic surfactant containing mixtures (51, 52).

The variations in the cmc, surface compositions, micelle compositions and structure are interpreted as a strong attractive synergistic interaction which is asymmetric with composition. The asymmetry and the changes in the interaction on the addition of electrolyte indicate a significant electrostatic and structural contribution to the interaction. Li et al (21) highlighted the change in the conformation of the zwitterion on the mixing of C_{12}SB with SDS as a major factor. The variations observed when changing from SDS to a methyl ester headgroup reinforce the importance of that structural change. At the air-water interface the strong interaction and the associated structural changes results in a significant enhancement in the total adsorption. The strength of the interaction is weaker but still significant in the micelle mixing compared to the surface mixing, due to the packing constraints being less significant in the micelles. However the synergistic interaction does result in micelle growth. Furthermore the micelle growth is substantially more pronounced in the presence of electrolyte. In electrolyte it is also strongly composition dependent and is most pronounced for equimolar solution compositions. These observations suggest a greater significance of the suppression of the electrostatic interactions on the micelle structure.

The results show how a comprehensive set of experimental data for mixed surfactants, encompassing variations in cmc, surface compositions and structure, enables a more detailed thermodynamic analysis which reveal the nature of the strong synergistic interaction. Also importantly it shows how the nature of the interaction between zwitterionic surfactants and co-surfactants can be manipulated to adjust and enhance surface adsorption and manipulate solution self-assembly properties. This provides exciting opportunities for a wide range of potential formulations. This is particularly relevant for personal care products and biological

applications, where mildness, reduced toxicity and improved biodegradability are important factors (5-12).

ACKNOWLEDGEMENTS

We acknowledge the provision of neutron beam time for the NR and SANS measurements at the ISIS Facility and for NR measurements at the Institute Laue Langevin, ILL. The invaluable scientific and technical support of the Instrument Scientists and support staff is acknowledged. The provision, through Najet Mahmoud and Stephen King, of some 'Xpress' beam time on LOQ and SANS2D at ISIS for some vital additional measurements is acknowledged. The DOI for the FIGARO data is doi:10.5291/ILL-DATA.9-10-1598.

AUTHOR CONTRIBUTIONS

The experimental design was made by KM, PXL, RKT and JP. The experimental measurements were made primarily by KM, ZW, YC and PXL, supported by the Instrument scientists, MC, JD, RD and AM at ISIS and the ILL. Different aspects of the data analysis were made by JP, RKT, PXL and KM. The paper was written and edited primarily by JP, RKT, KM and PXL, and all the authors have contributed to the final draft.

STATEMENT OF CONFLICTING INTERESTS

The authors are not aware of any conflicting or financial interests that would have influenced this study.

TABLE OF CONTENT GRAPHIC

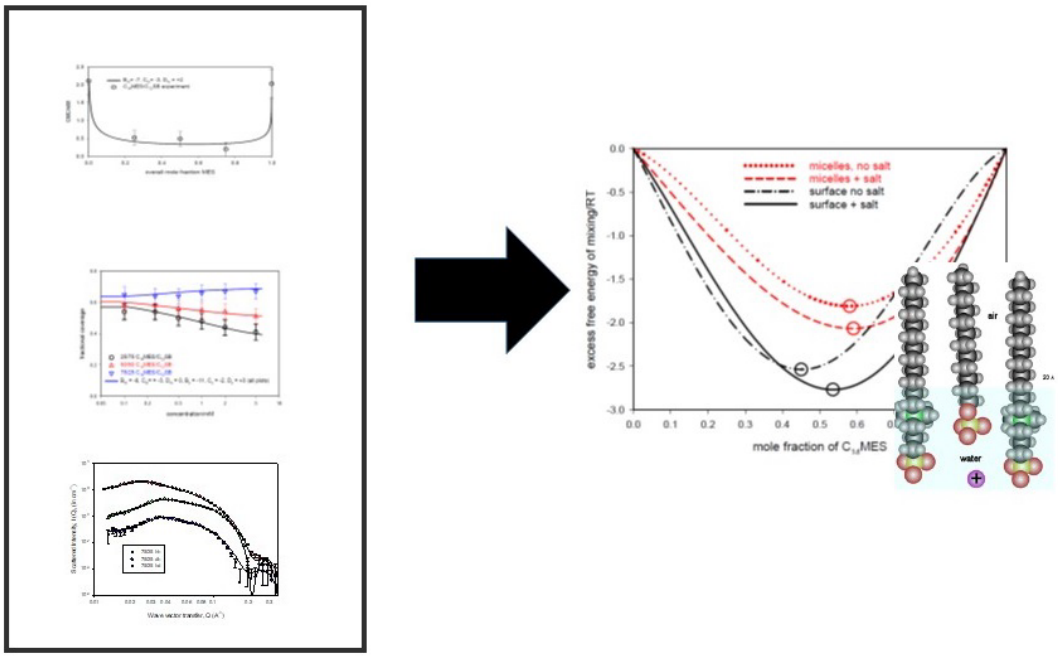

SUPPLEMENTARY INFORMATION

Supplementary data, in the form of figures and tables are included in the Supporting Information.

REFERENCES.

(1) R G Laughlin, Fundamentals of the zwitterionic group, Langmuir, 1991, 7, 842-847

(2) J G Weers, J F Rathman, F U Axe, C A Crichlow, L D Foyland, D R Scheuing, R J Wiersema, A G Zielske, Effect of intermolecular charge separation distance on the solution properties of Betaines and Sulfobetaines, Langmuir, 1991, 7, 854-867

(3) G Qu, J Cheng, J Wei, T Yu, W Ding, H Luan, Synthesis, characteristaion and surface properties of series of sulfobetaine surfactants, J. Surfact. Deterg. 2011, 14, 31-35

(4) D J Hodge, R G Laughlin, R H Ottewill, A R Rennie, Micellisation of ultralong chain surfactants, Langmuir, 1991, 7, 878-884

(5) G W Fernley, Zwitterionic surfactants, structure and performance, J. Am. Oil Chem. Soc. 1978, 55, 98-103

(6) B R Bluestein, C L Hilton, Eds. Amphoteric Surfactants, Surfactant Science Series 12, Marcel Dekker, NY, 1982

(7) L D Rhein, M Schlossman, A O'Lenick, P Somasundaran, Surfactants in personal care products and decorative cosmetics, 3rd Ed, CRC Press, Baton Rouge, USA, 2006

(8) M J L Castor, C Ojeda, A F Cirelli, Advances in surfactants for agrochemicals, Environ. Chem. Lett. 2014, 12, 85-95

(9) S Welling-Wester, M Feijlbrief, D G A M Koedijk, G W Welling, Detergent extraction of Herpes simplex virus type glycoprotein D by zwitterionic and nonionic detergents and purification by ion exchange high performance liquid chromatography, J. Chrom. A, 1998, 816, 29-37

(10) K D Danov, S D Kralchevska, P A Kralchevsky, K P Ananthapadmanabhan, A Lips, Mixed solutions of anionic and zwitterionic surfactants (betaines): surface tension isotherms, adsorption and relaxation kinetics, Langmuir, 2004, 20, 5445-5453

(11) A P Gerola, P F A Costa, F H Quina, H P Fiedler, F Nome, Zwitterionic surfactants in ion binding and catalysis, Curr. Opin. Coll. Int. Sci. 2017, 32, 39-47

(12) J Zhao, C Dai, A Ding, M Du, H Feng, Z Wei, A Chen, M Zhao, The structure effect on surface and interfacial properties of zwitterionic sulfobetaine surfactants for enhanced oil recovery, RSC Advances, 2019, 5, 13993

(13) K Tajima, A Nakamura, T Tsutui, Surface activity of complex mixed surfactant solutions, Bull. Chem. Soc. Japan, 1979, 52, 2060-2063

(14) M J Rosen, Synergism in mixtures containing zwitterionic surfactants, Langmuir, 1991, 7, 885-888

(15) T Iwasaki, M Ogawa, K Esumi, K Meguro, Interactions between Betaine type zwitterionic and anionic surfactants in mixed micelles, Langmuir, 1991, 7, 30-35

(16) J D Hines, R K Thomas, P R Garrett, G K Rennie, J Penfold, Investigation of mixing of binary surfactant solutions by surface tension and neutron reflection: strongly interacting anionic / zwitterionic mixtures, J. Phys. Chem. B, 1998, 102, 8834-8846

(17) F Li, G Z Li, J B Chen, Synergism in mixed zwitterionic-anionic surfactant solutions and the aggregation numbers of the mixed micelles, Coll. Surf. A, 1998, 145, 167-174

(18) P Wydro, M Paluch, A study of the interaction of dodecyl sulfobetaine with anionic and cationic surfactants in mixed micelles and monolayers at the air-water interface, J. Coll. Int. Sci. 2005, 286, 387-391

(19) D Lopez-Diaz, I Garcia-Mateos, M M Velazquez, Surface properties of mixed monolayers of sulfobetaines and ionic surfactants, J. Coll. Int. Sci. 2006, 299, 858-866

(20) A A McLachlan, D G Marangoni, Interaction between zwitterionic and conventional anionic and cationic surfactants, J. Coll. Int. Sci. 2006, 295, 243-248

(21) P Li, K Ma, R K Thomas, J Penfold, Analysis of the asymmetric synergy in the adsorption of zwitterionic-ionic surfactant mixtures at the air-water interface, below and above the cmc, J. Phys. Chem. B, 2016, 120, 3677-3691

(22) Y Zheng, X Lu, L Lai, H Yu, H Zheng, C Dai, The micelle thermodynamics and mixed properties of sulfobetaine type zwitterionic Gemini surfactants with nonionic and anionic surfactants, J. Mol. Liq. 2020, 299, 112108

(23) L Su, J Sun, F Ding, X Gao, L Zheng, Effect of molecular structure on synergism in mixed zwitterionic / anionic surfactant system: an experimental and simulation study, J. Mol. Liq. 2021, 322, 114933

(24) A Shiloach, D Blankschtein, Prediction of the cmc and synergies of binary surfactant mixtures containing zwitterionic surfactants, Langmuir, 1997, 13, 3968-3981

(25) M Mulqueen, D Blankschtein, Prediction of equilibrium surface tension and surface adsorption in aqueous surfactant mixtures containing zwitterionic surfactant, Langmuir, 2000, 16, 7640-7654

(26) A Goldsipe, D Blankschtein, Modelling counterion binding in ionic-nonionic and ionic-zwitterionic surfactant mixtures, Langmuir, 2005, 21, 9850-9865

(27) E Staples, J Penfold, I Tucker, Adsorption of mixed surfactants at the oil-water interface, J. Phys. Chem. B, 2000, 104, 606-614

(28) J R Lu, R K Thomas, J Penfold, Surfactant layers at the air-water interface: structure and composition, Adv. Coll. Int. Sci. 2000, 84, 143-304

(29) J Penfold, R K Thomas, Recent developments and applications of the thermodynamics of surfactant mixing, Mol. Phys. 2019, 117, 3376-3388

(30) J R Liley, R K Thomas, J Penfold, I M Tucker, J T Petkov, P Stevenson, J R P Webster, Surface adsorption in ternary surfactant mixtures, above the cmc: effects of asymmetry on the composition dependence of the excess free energy, J. Phys. Chem. B, 2017, 121, 2825-2838

(31) J R Liley, R K Thomas, J Penfold, I M Tucker, J T Petkov, P Stevenson, J R P Webster, Impact of electrolyte on adsorption at the air-water interface for ternary surfactant mixtures above the cmc, Langmuir, 2017, 33, 4301-4312

(32) J R Liley, R K Thomas, J Penfold, I M Tucker, J T Jordan, P Stevenson, I M Banat, R Marchant, M Rudden, J R P Webster, Adsorption at the air-water interface in biosurfactant-surfactant mixtures: a quantitative analysis of the adsorption in a 5-component mixture, Langmuir, 2017, 33, 13027-13039

(33) J J Scheibel, The evolution of anionic surfactant technology to meet the requirements of the laundry detergent industry, J. Surfact. Deterg. 2004, 7, 319-328

(34) H Xu, P X Li, K Ma, R J L Welbourne, J Penfold, D W Roberts, R K Thomas, J T Petkov, Adsorption of methyl ester sulfonate at the air-water interface: can limitations in the application of the Gibbs equation be overcome by 'computer purification', Langmiur, 33, 2017, 9944-9957

(35) H Xu, R K Thomas, J Penfold, P X Li, K Ma, R J L Welbourne, D W Roberts, J T Petkov, the impact of electrolyte on the adsorption of the anionic surfactant methyl ester sulfonate at the air-solution interface: surface multilayer formation, J. Coll. Int. Sci. 2018, 512, 231-238

(36) Z Wang, PX Li, K Ma, Y Chen, J Penfold, R K Thomas, D W Roberts, H Xu, J T Petkov, Z Yan, D A Venero, The structure of alkyl ester sulfonate surfactant micelles: the impact of different valence electrolytes and surfactant structure on micelle growth, J. Coll. Int. Sci. 2019, 557, 124-134

(37) SURF reflectometer at the ISIS neutron source, https://www.isis.stfc.ac.uk/instruments/ surf.aspx

(38) P Gutfreund, T Saerbeck, M A Gonzales, E Pellegrini, M Laver, C Dewhurst, R Cubitt, Towards generalised data reduction on a chopper-based time of flight instrument, J. Appl. Cryst. 2018, 51, 606-615

(39) LOQ diffractometer at the ISIS neutron source, https://www.isis.stfc.ac.uk/instrument pages/LOQ.aspx

(40) SANS2D diffractometer at the ISSI neutron source, https://www.isis.stfc.ac.uk/instrument pages/SANS2D.aspx

(41) LARMOR diffractometer at the ISSI neutron source, https://www.isis.stfc.ac.uk/instruments pages/LARMOR.aspx

(42) ZOOM diffractometer at the ISSI neutron source, https://www.isis.stfc.ac.uk/instrument pages/ZOOM.aspx

(43) R K Heenan, S M King, R Osborn, H B Stanley, RAL Internal Report, RAL-89-128, 1989

(44) J B Hayter, J Penfold, Determination of micelle structure and charge by small angle neutron scattering, Coll. Polym. Sci. 1983, 26, 1022-1030

(45) J B Hayter, J Penfold, An analytic structure factor for macroion solutions, Mol. Phys. 1981, 42, 109-118

(46) J B Hayter, J P Hansen, A rescaled mean spherical approximation structure factor for dilute charged colloidal dispersions, Mol. Phys. 1982, 46, 651-656

(47) P M Holland, D N Rubnigh, Non-ideal multicomponent mixed micelle model, J. Phys. Chem. 1983, 87, 1984-1990

(48) P M Holland, Non-ideal multicomponent mixed micelle model, Adv. Coll. Int. Sci. 1986, 26, 111-129

(49) J Penfold, E Staples, L Thompson, I Tucker, J Hines, R K Thomas, J R Lu, Solution and adsorption behaviour of the mixed surfactant system sodium dodecyl sulfate / n-hexaethylene glycol monododecyl ether, Langmuir, 1995, 11, 2496-2503

(50) H Xu, P X Li, K Ma, R Welbourne, J Doutch, J Penfold, R K Thomas, D W Roberts, J T Petkov, K T Choo, S Y Khoo, Adsorption and self-assembly in methyl ester sulfonate surfactants, their eutectic mixtures and the role of electrolyte, J. Coll. Int. Sci. 2018, 516, 456-465

(51) A Patist, S Devi, D O Shah, Importance of 1:3 molecular ratio on interfacial properties of mixed surfactant systems, Langmuir, 1999, 15, 7403-7405

(52) L Reif, P Somasundaran, Asymmetric excess free energies and variable interaction parameters in mixed micellisation, Langmuir, 1999, 15, 3411-3417

(53) P C Griffiths, A Paul, R K Heenan, J Penfold, R Ranganathan, B L Bales, the role of counterion concentration in determining micelle aggregation, J. Phys. Chem. B, 2004,108, 3810-3816

(54) Z Chen, J Penfold, P Li, Y Fan, Y Wang, J Doutch, Surface activity and aggregation behaviour of Gemini-like surfactants formed from SDS and diamines with hydrophobic and hydrophilic spacers, Soft Matter, 2017, 13, 8980-8989

(55) J Liley, J Penfold, R K Thomas, I Tucker, J Petkov, P S Stevenson, I Banat, R Marchant, M Rudden, A Terry, I Grillo, Self-assembly in dilute mixed surfactants and biosurfactant-surfactant mixtures, J. Coll. Int. Sci. 2017, 487, 493-503

(56) I Grillo, J Penfold, Self-assembly in mixed anionic-nonionic surfactants in aqueous solution, Langmuir, 2011, 27, 7453-7463

(57) J Penfold, I Tucker, R K Thomas, E Staples, R Schuerman, The structure of mixed anionic-nonionic surfactant micelles: experimental observations relating to the role of headgroup electrostatics and steric effects and the effect of electrolyte, J. Phys. Chem. B, 2005, 109, 10760-10770